Interactions of Myogenic bHLH Transcription Factors with Calcium-Binding Calmodulin and S100a (αα) Proteins[†,▽]

Jacques Baudier,*[,‡] Evelyne Bergeret,[‡] Nathalie Bertacchi,[‡] Harold Weintraub,[§] Jean Gagnon,[∥] and Jerome Garin[⊥]

Département de Biologie Moléculaire et Structurale, CEA, DBMS-BMCC, INSERM Unité 309, and Laboratoire de Chimie des Proteines, CEA, DBMS-CP, CEN-G, 38054 Grenoble, France, Institut de Biologie Structurale, CEA and CNRS, 38027 Grenoble, France, and Department of Genetics, Fred Hutchinson Cancer Research Center, Seattle, Washington 98104

Received October 21, 1994; Revised Manuscript Received April 11, 1995[⊗]

ABSTRACT: MyoD belongs to a family of myogenic basic helix−loop−helix (bHLH) transcription factors that activate muscle-specific genes. The basic helix I sequence of the bHLH motif contains a consensus sequence for protein kinase C (PKC) substrates. We show here that MyoD is indeed phosphorylated by PKC *in vitro* on Thr 115 within the basic part of the bHLH motif. By analogy with calmodulin-target peptide models, we also identified within the consensus basic helix I motif of myogenic proteins a conserved putative calmodulin/S100-binding domain. Calcium-dependent interaction between MyoD with calmodulin and the abundant muscle S100a(αα) proteins was demonstrated by affinity chromatography and cross-linking experiments. The binding of calmodulin and S100a inhibited MyoD phosphorylation by PKC as well as MyoD DNA binding activity. S100a was found to be more efficient than calmodulin in antagonizing DNA binding to MyoD. We next developped a rapid purification method for bacterial recombinant MyoD-bHLH domain by affinity chromatography using a calmodulin−Sepharose column and investigated the phosphorylation of that peptide by PKC and its interactions with calmodulin and S100a. We confirmed the phosphorylation of the threonine residue 115 in the MyoD-bHLH by PKC with a K_m of 0.8 μM. Calmodulin and S100a binding inhibited MyoD-bHLH phosphorylation by PKC. A strict calcium-dependent interaction between calcium binding proteins and the MyoD-bHLH was identified by native gel electrophoresis and fluorescence spectroscopy with 5-(dimethylamino)naphthalene-1-sulfonylcalmodulin. The MyoD-bHLH bound to fluorescently labeled 5-(dimethylamino)naphthalene-1-sulfonylcalmodulin with a dissociation constant around 20 nM. S100a inhibited stoichiometrically the binding of the bHLH peptide for labeled calmodulin, suggesting an affinity of S100a for the bHLH peptide at least 1 order of magnitude higher than calmodulin. In favor of an *in vivo* interaction between S100a and MyoD, we report that S100a- and MyoD-like immunoreactivities colocalize in H9c2 cells, and that a significant amount of MyoD-like immunoreactivity is recovered in the S100a immunoprecipitate from crude H9c2 cell extract in the presence of calcium. We propose that myogenic proteins represent a new family of calmodulin/S100-binding PKC substrates and that calmodulin/S100a could participate in the regulation of the bHLH myogenic protein activities.

Calmodulin (CaM),[1] the major EF-hand calcium binding protein (CaBP), is a ubiquitous and multifunctional Ca^{2+}-dependent regulator that binds and activates more than 20 enzymes in eukaryotic cells [for a review on the EF-hand family of CaBPs, see Persechini et al. (1989)]. *In vitro*, CaM also interacts with and modulates the phosphorylation of a number of cytosolic PKC substrates. Two families of PKC substrates that bind CaM *in vitro* have been identified, the MARCKS brothers proteins (Aderem 1992; Blackshear 1993) and their relatives the neuromodulin/neurogranin proteins (Alexander et al., 1988; Baudier et al., 1991). Members of each family are characterized by a conserved sequence of 17−20 amino acids that corresponds to the PKC phosphorylation site domain and the CaM binding domain.

Within the EF-hand CaBP superfamily, a distinct set of proteins is collectively given the name of S100 proteins. At least 12 S100 proteins have been identified that are expressed in a cell-type-dependent fashion [for reviews on S100 proteins, see Kligman and Hilt (1988) and Hilt and Kligman (1991)]. Several S100 genes are clustered on human chromosome 1q21, and mRNAs encoding these proteins are generally expressed during a specific cell growth stage, suggesting that S100 proteins may play roles in mediating the functions of Ca^{2+} in the control of the cell cycle and/or in cell differentiation (Hilt & Kligman, 1991; Engelkamp et al., 1993). In line with a role of S100 protein in cell differentiation, the specific expression of the S100a species during early embryonic development has been recently

[†] This work was supported by grant from Association Française Contre les Myopathies and Association pour la Recherche sur le Cancer to J.B.

[▽] This work is dedicated to Harold Weintraub whose scientific spirit has made this study possible.

* To whom correspondence should be addressed: Département de Biologie Moléculaire et Structurale, INSERM Unité 244, DBMS-BRCE, CEN-G, 17 rue des Martyrs, 38054 Grenoble Cedex 9, France. Telephone: (33) 76 88 43 28. Fax: (33) 76 88 51 00.

[‡] Département de Biologie Moléculaire et Structurale, CEA.

[§] Fred Hutchinson Cancer Research Center.

[∥] Institut de Biologie Structurale, CEA.

[⊥] Laboratoire de Chimie des Proteines, CEA.

[⊗] Abstract published in *Advance ACS Abstracts,* June 1, 1995.

[1] Abbreviations: CaM, calmodulin; DANS, 5-(dimethylamino)-naphthalene-1-sulfonyl; EDTA, ethylenediaminetetraacetic acid; EGTA, ethylene glycol bis(β-aminoethyl ether)-*N,N,N′,N′*-tetraacetic acid; HEPES, *N*-(2-hydroxyethyl)piperazine-*N′*-2-ethanesulfonic acid; MARCKS, myristoylated alanine-rich C kinase substrates; PKC, protein kinase C; PMSF, phenylmethanesulfonyl fluoride; SDS, sodium dodecyl sulfate.

0006-2960/95/0434-7834$09.00/0

reported (Ivanenkov et al., 1993), and it has been suggested that S100b might be involved in the maturation and differentiation of glial cells (Labourdette & Mandel, 1978).

Two members of the S100 protein family, S100a and S100b, have been extensively studied at the biochemical level (Baudier & Gerard, 1986; Baudier et al., 1986a,b). S100a and S100b are non-covalent dimers (M_r 20 000) with subunit compositions $\alpha\alpha$ and $\beta\beta$, respectively. Similarities of S100a and S100b in interacting with CaM-target proteins, peptides, and drugs have been reported (Marshak et al., 1981; Albert et al., 1984, Baudier et al., 1987; Baudier & Cole, 1988; Fano et al., 1988), suggesting that S100a/b and CaM have a common structural domain which could mediate an interaction with common target proteins (Baudier et al., 1987). Although the exact functions of the different S100 protein species remain unclear, most of the putatively identified S100-target proteins are phosphoproteins. The various demonstrated effects of the S100 proteins in cell cycle progression and cell-type differentiation may thus be mediated by the same basic processes, i.e., interaction with protein kinase substrates and modulation of target protein kinase substrate phosphorylation (Kligman & Hilt, 1988; Deloulme et al., 1989; Hagiwara et al., 1988; Baudier et al., 1992). The identification of S100-target proteins is essential to the determination of the exact S100 protein functions.

The phosphoprotein MyoD (Tapscott et al., 1988), a member of a family of myogenic transcriptional regulatory proteins including myogenin (Wright et al., 1989), Myf-5 (Braun et al., 1989) and MRF4 or herculin (Miner & Wold, 1990), can regulate mammalian skeletal muscle development [for reviews, see Olson (1990) and Weintraub et al. (1991)] and also contributes to many of the other aspects of the muscle phenotype in the adult (Merlie et al., 1994). Members of the MyoD family are characterized by a conserved multifunctional 70 amino acid sequence that encompasses a basic region (b) and an adjacent helix−loop−helix (HLH) motif identified for myogenic specificity (Davis et al., 1990). The shared bHLH motif is a multifunctional and regulatory domain that accounts for the common property of this protein family, which is the ability to bind to an E-box DNA consensus sequence (CANNTG) as homodimers and heterodimers (Davis et al., 1990). In MyoD, the bHLH motif mediates dimerization and promotes heterodimer formation with other regulatory proteins such as the E2A gene products and the Id proteins that respectively potentiate or inhibit DNA binding activity of myogenic proteins (Benezra et al., 1990). A report has also shown that bFGF-mediated phosphorylation of myogenin by PKC at a conserved Thr residue within the basic domain in the bHLH motif inactivates myogenin (Li et al., 1992). The conserved PKC phosphorylation site on myogenic proteins matches perfectly the proposed consensus PKC phosphorylation site (Kennelly & Krebs, 1991). Moreover, we find that this motif ressembles in some respect the PKC phosphorylation site on CaM/S100-binding PKC substrates of the neurogranin/neuromodulin family (Table 1). The basic helix I sequence within the bHLH motif of myogenic proteins also presents striking homology with CaM binding domains on CaM-dependent enzyme (see Table 1).

In this work we characterize MyoD as a PKC substrate and identify the PKC phosphorylation sites. We also provide evidence that the MyoD bHLH domain is directly involved in the Ca^{2+}-dependent interactions of MyoD with the calcium binding proteins CaM and S100a($\alpha\alpha$), an S100 species abundantly expressed in cardiac and skeletal muscles (Kato et al., 1986; Haimoto & Kato, 1987, 1988; Zimmer, 1991; Engelkamp et al., 1992). The high-affinity interactions between calcium binding proteins and MyoD bHLH, in the nanomolar range, make our observation physiologically significant and strongly support the idea that myogenic proteins represent a new family of calmodulin/S100-binding PKC substrates.

MATERIALS AND METHODS.

Proteins and Enzymes. CaM, S100b, and S100a were purified from bovine brain as previously described (Baudier et al., 1982; Baudier & Gerard, 1986). CaM, S100b, and S100a were coupled to Sepharose in their Ca^{2+}-bound states as previously described (Baudier et al., 1987). CaM, S100b ($\beta\beta$), and S100a ($\alpha\alpha$) protein concentrations were measured by UV absorption spectroscopy, assuming absorption coefficients of 3300, 3400, and 18 500 M^{-1} cm^{-1}, respectively. 5-(Dimethylamino)naphthalene-1-sulfonylcalmodulin was obtained from Sigma.

Recombinant MyoD was expressed in *E. coli* using the T7 expression system developed by Studier and Moffat (1986). The detailed purification for the recombinant MyoD protein will be described elsewhere. The purified MyoD protein was stored in aliquots at −20 °C in 40 mM HEPES, pH 7.5, 150 mM NaCl, and 5 mM DTT. Only fresh protein preparations were used. Upon long-term storage and repeated thawing, properties of the MyoD protein were altered: PKC phosphorylation stoichiometry, DNA binding activity, and Coomassie blue binding decreased significantly. We attributed these changes to intrachain disulfide bond formation within the protein.

Recombinant MyoD bHLH (Starovasnik et al., 1992) contains the entire bHLH region starting at residue 102 plus three amino acids at the N-terminus corresponding to the native N-terminus of mouse MyoD. For purification of the recombinant MyoD bHLH, bacteria containing the MyoD bHLH plasmid were grown as described in Starovasnik et al., (1992). Cells were lysed by freeze-thawing and sonication in the presence of lysis buffer containing 50 mM Hepes, pH 7.6, 0.1 M KCl, 10 mM DTT, 1 mM PMSF, 10% glycerol, and 0.1% Triton X-100. The cell extract was centrifuged at 20000*g* for 1 h, and the supernatant was adjusted to 0.3% polyethylenimine and stirred for 1 h at 4 °C to precipitate nucleic acids. After centrifugation at 20000*g* for 30 min, the supernatant was sequentially precipitated with 40% and 80% ammonium sulfate. The 80% ammonium sulfate pellet, which contained MyoD bHLH, was rapidly washed with water and resuspended in 20 mM Hepes, pH 7.6, 0.5 M NaCl, and 10 mM DTT (buffer A) plus 0.5 mM $CaCl_2$. MyoD bHLH solution (8 mL, 1.5 mg/mL) was applied to an 8-mL CaM-Sepharose column equilibrated with buffer A plus 0.5 mM $CaCl_2$. After extensive washing with equilibrating buffer, MyoD bHLH was eluted from the column with buffer A containing 1 mM EGTA. Column fractions were pooled, and final purification was achieved by reverse-phase FPLC using a ProRPC column with a water/acetonitrile gradient in the presence of 0.1% TFA. MyoD bHLH eluted at about 29−30% acetonitrile. Column fractions were extensively dialyzed against 40 mM Tris-HCl, pH 7.6, and 0.2 M NaCl. After protein determination, 10 mM DTT was added to the protein solution and the preparation was stored at −20 °C.

Table 1: Comparison between the CaM Binding Domain on CaM Target Enzymes and CaM/S100 Binding PKC Substrates with the Basic α Helix I Motif on the Myogenic Proteins MyoD and Myogenin[a]

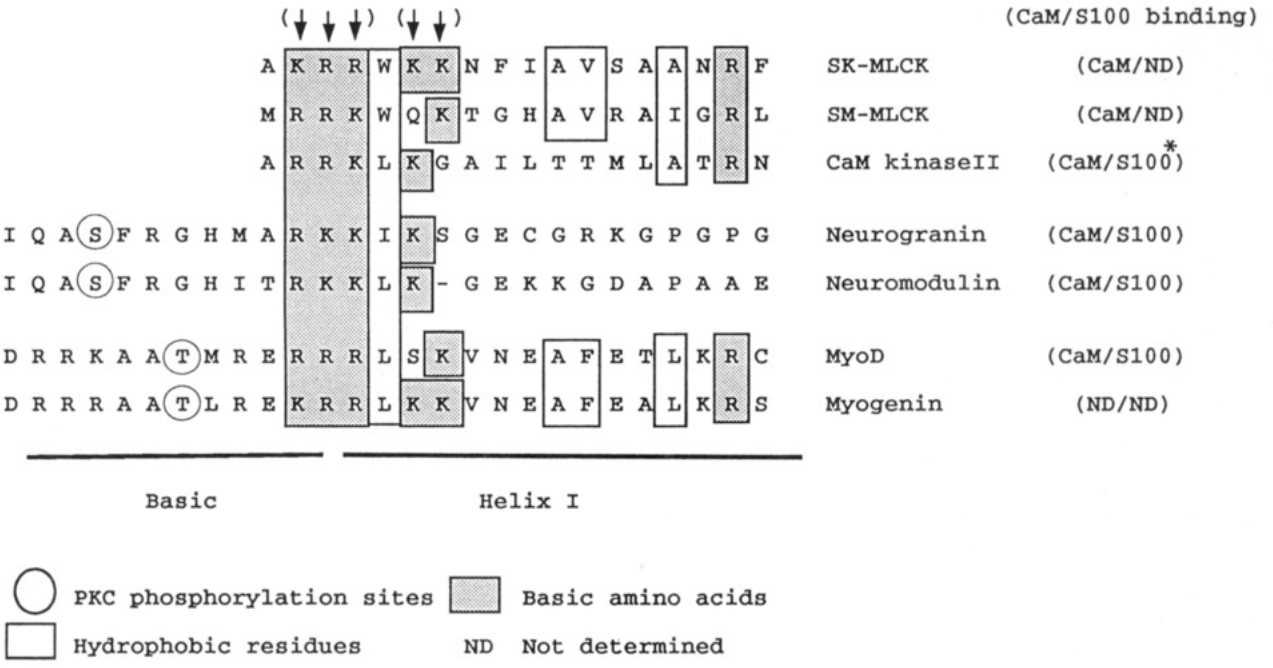

[a] Multidimensional H-NMR and crystallographic studies of the complexes between CaM with peptides comprising the CaM binding domain indicated that CaM binds to basic amphipathic α-helices using a combination of hydrophobic and electrostatic interactions (Ikura et al., 1992; Meador et al., 1992). The α-helix I motif in myogenic proteins has in common with the CaM-binding domain of CaM-target enzymes the presence of aromatic or aliphatic residues (white boxes) critical for hydrophobic interaction with the carboxyl-terminal domain of CaM and for high-affinity interactions (Bagchi et al., 1992; Ikura et al., 1992; Meador et al., 1992). The carboxy-terminus of the CaM binding domain on CaM-target enzymes also has an arginine residue that was found to be critical for CaM binding (Bagchi et al., 1992); this residue is also present in the putative CaM binding domain of myogenic proteins. Note also the presence of a cluster of basic amino acids (arrows) present in all CaM-target peptides and myogenic proteins. This basic cluster was shown to be essential for high-affinity CaM binding by directed mutagenesis (Fitzsimons et al., 1992; Herring, 1991). The basic motif in myogenic proteins also harbors a conserved Thr residue within a perfect consensus sequence for PKC phosphorylation (Kennelly & Krebs, 1991). The PKC phosphorylation site domain on myogenic proteins shows similarities with the PKC and CaM/S100 binding domain on neurogranin and neuromodulin. ND, not determined. *In this case S100b binding to CaM kinase II stimulates neither autophosphorylation of the enzyme nor significantly the phosphorylation of its substrates (unpublished data).

MyoD and MyoD bHLH concentrations were determined with the Coomassie blue method (Bio-Rad assay kit) using bovine albumin as a standard.

Rat brain type II PKC was purified as described by Pelosin et al. (1987). Protein kinase C and sequencing grade trypsin were from Boehringer.

Antibodies. Rabbit antibodies against the C-terminus of MyoD (residues 160−307) were used for immunoprecipitation (Tapscott et al., 1988). Hybridoma supernatant, 5.8A, containing a monoclonal anti-MyoD was used for Western blot analysis. Rabbit antibodies against purified S100a were used for immunoprecipitation. These antibodies recognize specifically the purified S100α-subunit on Western blot (1:2000−1:1000 dilutions) but do cross react at low dilution (1:500) with the S100β-subunit, which has approximately 50% sequence homology with S100α.

Protein Kinase Assays. Purified MyoD (0.5−5 μg) was diluted in protein kinase buffer containing 20 mM HEPES−NaOH, pH 7.5, 5 mM $MgCl_2$, and 1 mM DTT and including 40−200 μM ATP. CKII phosphorylation reactions were initiated by the addition of 0.3 μg of enzyme. For reactions using rat brain type II PKC, 0.1 mM Ca^{2+} and emulsified lipids (20μg/mL phosphatidylserine, 1μg/ml diacylglycerol) were added. The phosphorylation reactions were performed at 30 °C.

Phosphorylation reactions with MyoD bHLH were performed in the same manner as for MyoD, except that purified rat brain PKC from a commercial source was used at the concentration of 0.1 μg/mL. ^{32}P incorporation was monitored by spotting aliquots of the reaction mixture onto 1-cm^2 pieces of Whatman P81 paper, which were washed three times with 30% acetic acid and dried; the radioactive label was then counted in a liquid scintillation counter.

Determination of the PKC Phosphorylation Site on MyoD. MyoD, 800 μg in 800 μL of standard reaction buffer, was phosphorylated with type II PKC, in the presence of [^{32}P]-ATP. After 20 min, the phosphorylation stoichiometry reached about 0.1 mol of phosphate incorporated per mol of MyoD. The protein was then precipitated in 10% TCA, and the pellet was washed twice with ethanol and resuspended in 200 μL of formic acid plus 10% H_2O_2. After 1 h at 4 °C, the oxidized protein was diluted 5-fold in water and lyophilized. The protein was resuspended in SDS buffer and run on a 10% SDS−PAGE gel, and the ^{32}P-labeled MyoD was electroeluted from the gel in 50 mM Tris-HCl, pH 8.5, and 0.1% SDS. The electroeluted ^{32}P-labeled MyoD (200 μg in 600 μL) was mixed with an equal amount of non-phosphorylated MyoD, precipitated with 20% TCA, and resuspended in 500 μL of buffer containing 100 mM Tris-HCl, pH 8. The protein was digested with trypsin (1:10, weight ratio). After 18 h at 32 °C, the sample was adjusted to 0.1% trifluoroacetic acid and applied to a Pep-RPC column connected to an FPLC chromatograph equiped with a 214-nm UV recorder. The peptides were separated with a

gradient of 0−50% acetonitrile in 0.1% TFA in 30 min at a flow rate of 0.5 mL/min. Fractions (0.5 mL) were collected, and the radioactivity of each fraction was determined by Cerenkov counting. A major symmetrical radioactive peak eluted from the column between 11 and 12.5% acetonitrile. To improve the purity of the phosphorylated phosphopeptide, the radioactive fractions were recycled, after lyophylization, on the Pep-RPC column eluted with a gradient of 0−15% acetonitrile and 0.1% TFA in 20 min. Under these conditions the phosphopeptide eluted between 7 and 7.5% acetonitrile. The fraction corresponding to the peak of radioactivity was subjected to amino acid sequence analysis.

Determination of the PKC Phosphorylation Sites on MyoD bHLH. MyoD bHLH (100 μg) was phosphorylated by PKC from a commercial source, and the phosphorylated peptide were purified by reverse-phase FPLC. Prior to sequencing, the peptide was covalently immobilized on Sequelon arylamine disks (Millipore) as described by Garin et al. (1994). The total applied radioactivity was 50 000 cpm, and the coupling yield was 85%. The disk was placed in the protein sequencer (Applied Biosystem 477A coupled to an HPLC 120A chromatography system). Radioactivity elution was optimized by introducing extensive washing of the Sequelon membrane with methanol and TFA in the sequencer program to avoid excessive carry-over of $^{32}P_i$ from one amino acid residue to the next. Radioactivity recovered after each Edman degradation cycle was determined by liquid scintillation. The values were corrected from the average repetitive yield of the sequence analysis, which was calculated to be 92%.

DNA Binding Assays. Recombinant MyoD DNA binding activity was measured by gel retardation using a ^{32}P-labeled oligonucleotide probe encompassing the right E-Box from the mouse MCK enhancer. The sequence of the oligonucleotide is GATCCCCCCAACACCTGCTGCCTGA, read 5′ to 3′ toward the MCK promoter. The gel-purified double-stranded oligonucleotide was labeled by using the kinase reaction using [γ-^{32}P]ATP (3000 Ci/ mmol; Amersham). MyoD (0.01 mg/mL) was diluted in DNA binding buffer containing 20 mM Hepes, pH 7.6, 50 mM KCl, 1 mM DTT, 5% glycerol, and 100 ng of poly(dAdT) plus 0.2 mM $CaCl_2$ or 1 mM EDTA and CaBPs as indicated in the figure captions. One nanogram of the labeled probe was then added in a final volume of 20 μL. The mixture was left at room temperature for 5 min, loaded on a 5% non-denaturing polyacrylamide gel, and run in a buffer containing 10 mM Hepes, 10 mM Tris, and 0.1 mM $CaCl_2$, pH 8.

Native Gel Electrophoresis. Gels containing 13% acrylamide, 0.375 M Tris-HCl, pH 8.3, and 0.5 mM $CaCl_2$ or 1 mM EGTA were prepared without stacking gels. MyoD bHLH peptide and CaBPs were incubated in 40 mM Tris-HCl, pH 8, 0.2 M NaCl, 5 mM DTT, 15% glycerol, and 0.5 mM $CaCl_2$ or 1 mM EGTA for 5 min on ice prior to electrophoresis. The gels were run at 20 mA. The electrode buffer consisted of 25 mM Tris, 192 mM glycine, and 0.5 mM $CaCl_2$ or 1 mM EGTA. The gels were stained with Coomassie blue.

Fluorescence Measurements. The fluorescence measurements were performed with a Perkin-Elmer spectrofluorometer. Tris-HCl, 50 mM at pH 8, and 0.12 M NaCl containing either 0.1 mM $CaCl_2$ or 2 mM EGTA was used to buffer the system. For titration experiments, excitation was at 345 nm and emission was monitored at 475 nm.

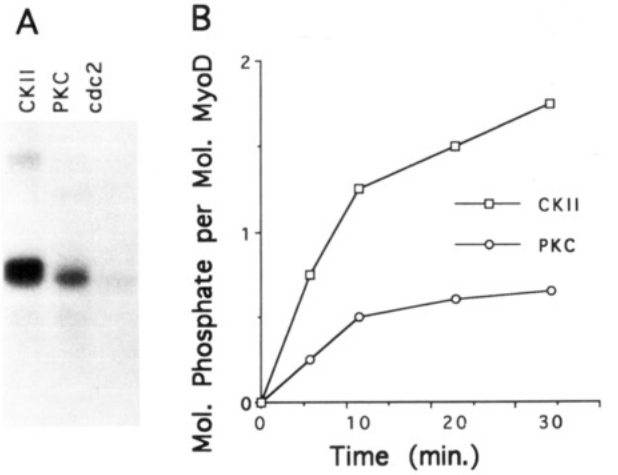

FIGURE 1: Phosphorylation of MyoD by PKC and CKII. (A) Autoradiograms showing the phosphoprotein patterns observed after steady-state phosphorylation of recombinant MyoD by CKII, PKC, and cdc2. (B) Comparison of the time course and stoichiometry of MyoD phosphorylation by PKC and CKII. MyoD was incubated in the presence of type II PKC or CKII in standard kinase assay conditions.

Immunofluorescence. H9c2 cells (Kimes & Brandt, 1976) were grown on glass coverslips, fixed with 4% paraformaldehyde in PBS, permeabilized with −20 °C methanol for 5 min on ice, and stained either for MyoD or for S100a with the corresponding rabbit sera at 1:200 dilution in PBS and rhodamine-conjugated second antibody. In control experiments, sera were preincubated with purified MyoD or S100a proteins (0.5 mg/mL) overnight at 4 °C.

Immunoprecipitation. Approximately 4×10^7 exponentially growing H9c2 cells were lysed in 2 mL of 20 mM Tris-HCl, pH 7.5, 0.2 M NaCl, 0.2% NP40, 3 mM Pefabloc, 20 μM aprotinin, 10 μM amastatin, and 20 μM pepstatin. After sonication and centrifugation to remove insoluble material, the supernatant was adjusted to 0.1 mM $CaCl_2$. Ten microliters of anti-MyoD serum or anti-S100a serum, or 10 μL of anti-neuromodulin serum used as control, was added, followed by 20 μL packed volume of protein A-agarose. The samples were shaken for 1 h at 4 °C, followed by three washes in lysis buffer plus 0.1 mM $CaCl_2$. Samples were then heated to 90 °C for 5 min in SDS gel sample buffer and loaded onto a 10% SDS−PAGE gel. The gel was transferred onto a nitrocellulose membrane followed by immunoblot analysis with a mouse monoclonal antibody, 5.8A, against MyoD.

RESULTS

Phosphorylation of MyoD by PKC. By analogy with a proposed consensus PKC phosphorylation site (Kennelly & Krebs, 1991) and the PKC phosphorylation domains on neurogranin and neuromodulin (Baudier et al., 1991), a putative protein kinase C phosphorylation site can be predicted within the basic region of the MyoD gene family (Table 1).

In vitro phosphorylation of recombinant MyoD by purified type II PKC confirmed that MyoD is a PKC substrate (Figure1A). As expected, phosphorylation of MyoD by type II PKC is totally calcium- and phospholipid-dependent (not shown). In our assay conditions, a stoichiometry of 0.5−0.6 mol of phosphate incorporated per mol of protein was obtained, suggesting a single phosphorylation site on the

protein (Figure 1B). Phosphoamino acid analysis by thin-layer chromatography of the HCl-hydrolyzed ^{32}P-labeled MyoD revealed the presence of mainly phosphothreonine. The phosphorylation site sequence was determined after tryptic digestion of the ^{32}P-phosphorylated protein and automatic sequencing of the major radioactive peptide (see Materials and Methods for details). Amino acid sequence analysis of this phosphopeptide revealed the sequence KAATMR where the single threonine residue is the only candidate for phosphorylation. This residue corresponds to Thr 115 within the basic part of the bHLH motif (Table 1), and is homologous to the PKC-phosphorylated Thr 87, identified on myogenin (Li et al., 1992). The fact that trypsin cleaved phosphorylated MyoD at Arg 111 but not at Lys 112 could be due to an effect of the phosphate group on the accessibility of Lys 112 to the enzyme.

Three other kinases were tested for their ability to use MyoD as substrate, casein kinase II (CKII), cycline B-cdc2 kinase (cdc2), and the calmodulin-dependent kinase II. Only CKII and cdc2 phosphorylated MyoD to different extents (Figure 1A). The phosphorylation of myogenin by CKII has been observed also (Li et al., 1992).

In our assay conditions CKII in its oligomeric form ($\alpha 2\beta 2$) incorporated up to 1.5−1.7 mol of phosphate per mol of protein (Figure 1B) mainly on serine residues. Unlike PKC, CKII induced a shift of the protein migration toward the cathode, as has been observed also for cellular MyoD (Tapscott et al., 1988; Mitsui et al., 1993) (Figure 1A). A detailed study on the phosphorylation of MyoD by CKII is in preparation (C. Cochet, O. Filhol, and J. Baudier, manuscript in preparation). It is interesting to note that chicken MyoD from muscle cultures or produced in sf9 cells is hyperphosphorylated exclusively on serine residues and migrates with lower electrophoretic mobility compared to the dephosphorylated proteins (Mitsui et al., 1993), suggesting that the residues phosphorylated *in vitro* by CKII are probably also phosphorylated *in vivo*.

Interactions of MyoD with S100 and CaM Proteins. A putative CaM/S100 binding domain can also be predicted within the basic helix I motif on myogenic proteins (Table 1). Several studies have shown that typical CaM binding domains comprise peptide sequences with a high propensity for amphipathic α helix formation and the presence of a series of basic amino acids interspersed within hydrophobic residues (Ikura et al., 1992; Meador et al., 1992). The patterns of hydrophilic and hydrophobic residues required for binding the carboxyl-terminal domain of CaM (Ikura et al., 1992) are comparable for MyoD/myogenin and CaM-target peptides. There is also a striking similarity between the positions of a basic amino acid cluster at the begining of the α helix motifs. These basic residues, which interact with acidic residues in CaM, have been found to be essential for high-affinity CaM binding to target enzymes (Fitzsimons et al., 1992). This cluster of basic residues is also found within the consensus CaM binding domain and PKC phosphorylation domain of the brain-specific CaM binding PKC substrates neuromodulin and neurogranin (Apel et al., 1991; Baudier et al., 1991), thus confirming its essential role in CaM binding in general.

To confirm a functional homology between the basic helix I motif on MyoD and a CaM/S100 binding motif, we examined the binding of MyoD to CaM and S100 proteins and the effect of such an interaction on the basic properties

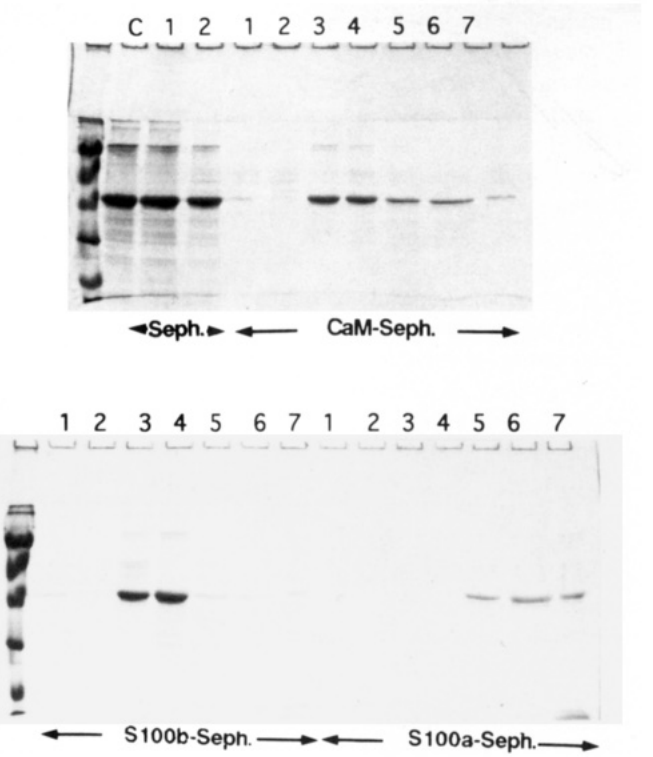

FIGURE 2: Ca^{2+}-dependent affinity chromatography of purified MyoD on CaM-, S100b-, and S100a-Sepharose columns. 12% SDS−PAGE analysis and Coomassie blue staining of the MyoD protein eluted from Sepharose CL4B, CaM-Sepharose, S100b-Sepharose and S100a-Sepharose columns as indicated. MyoD protein (0.7 mL, 1.2 mg/mL) in 40 mM Tris-HCL, pH 7.5, 0.2 M NaCl, and 5 mM DTT (buffer A) plus 0.5 mM $CaCl_2$ was applied on 2-mL columns equilibrated with buffer A plus 0.5 mM $CaCl_2$; the columns were first washed with 10 column volumes of the equilibrating buffer and then with 10 column volumes of buffer A containing 4 mM EGTA followed by 10 column volumes of buffer A containing 4 mM EGTA plus 0.5 M NaCl. One-milliliter fractions were collected. The columns were additionally washed with 5 M guanidinium chloride to elute the residual bound proteins. Only the two fractions eluted from the columns that have the highest protein content were analyzed. Lanes 1 and 2, protein eluted with buffer A plus 0.5 mM $CaCl_2$; lanes 3 and 4, protein eluted with buffer A plus 4 mM EGTA; lanes 5 and 6, protein eluted with buffer A containing 0.5 M NaCl plus 4 mM EGTA; lanes 7, protein eluted with 5 M guanidinium chloride. Lane C is the purified MyoD. On the left side of the gels are the molecular mass standards, 94 000, 69 000, 46 000, 30 000, and 20 000 from top to bottom.

of MyoD *in vitro*. We also extended this study to the characterization of the interaction of CaM and S100a with the consensus bHLH domain common to myogenic proteins.

MyoD binding to S100b, S100a or CaM was first studied by affinity chromatography using S100b-, S100a-, or CaM-Sepharose columns. Figure 2 shows the SDS−PAGE analysis of the protein fractions eluted from the columns and stained with Coomassie blue. There was no binding of MyoD to a Sepharose CL4B column used as a control. In the presence of $CaCl_2$ all MyoD protein remained bound to the CaM-, S100b-, and S100a-Sepharose columns (lanes 1−2), indicating that in their Ca^{2+}-bound conformations the CaBPs interact with MyoD. All the MyoD bound to the S100b-Sepharose eluted from the column with buffer containing EGTA and 0.2 M NaCl (lanes 3 and 4), indicating a strict Ca^{2+}-dependent interaction between the two proteins. At the same salt concentration a significant amount of MyoD remained bound to the CaM column and was eluted at higher salt concentrations, i.e., 0.5 M NaCl (lanes 5 and 6). This

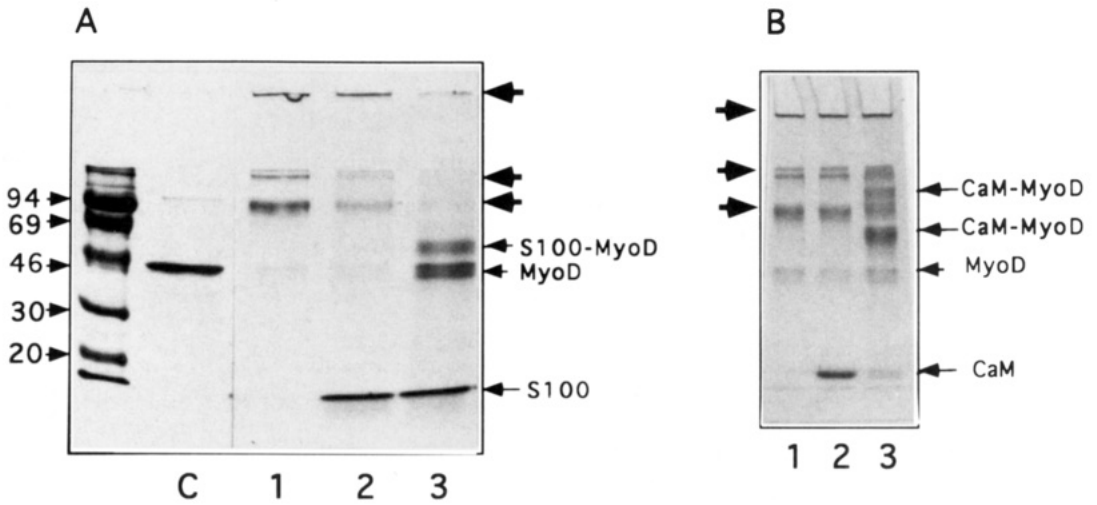

FIGURE 3: Cross-linking between MyoD with the S100a subunit and CaM. To visualize complex formation between MyoD and CaBPs, the proteins were mixed in 20 mM HEPES, pH 7.5, and 150 mM NaCl and incubated with 5 mM of the hetero-bifunctional reagent *bis*(sulfosuccinimidyl) suberate at 30 °C for 15 min. The cross-linked proteins were analyzed by 12% PAGE and Coomassie blue staining. Panel A: MyoD (15 μM) was incubated in the absence (lane 1) or in the presence of S100a (molar ratio S100a:MyoD = 3) plus EGTA (lane 2) or $CaCl_2$ (lane 3). In the left margin are molecular mass standards (kDa), and in lane C is purified MyoD. Panel B: Myo D was incubated in the absence (lane 1) or in the presence of CaM (molar ratio CaM:MyoD = 2) plus EGTA (lane 2) or $CaCl_2$ (lane 3). In panels A and B, large arrows indicate position of cross-linked MyoD dimer, tetramer, and higher MyoD aggregates that do not penetrate the staking gel. Positions of the S100a-α subunits or CaM and of heterocomplexes between MyoD and the S100a-α subunits or CaM are also indicated.

indicated that the Ca^{2+}-dependent interaction between MyoD and CaM was fully reversible but also that Ca^{2+}-independent interaction can occur between MyoD and CaM-Sepharose. Ca^{2+}-independent association between MyoD and the S100a coupled to Sepharose was also observed since most of the MyoD protein remained bound to the S100a-Sepharose column after washing with EGTA and 0.2 M NaCl. MyoD eluted from the S100a column with EGTA containing buffer plus 0.5 M NaCl as a broad protein peak. Some remained bound to the column and eluted with 5 M guanidinium chloride (lane 7).

Dilution of the MyoD protein 100-fold did not modify the binding of the protein to the CaM-Sepharose column (not shown).

The binding of MyoD to CaBPs was confirmed by covalent cross-linking experiments of the protein complexes with the hydrophilic heterobifunctional reagent bis(sulfosuccinimidyl) suberate (BS^3), a water-soluble analogue of disuccinimidyl suberate (DSS) (Figure 3).

In the absence of CaBP (lanes 1) or in the presence of the individual CaBPs plus EGTA (lanes 2) covalent cross-linking occurred between MyoD molecules. This was shown by the presence of dimer and higher molecular weight polymers on SDS−PAGE, indicating that, at the concentration used, the protein may self-aggregate in solution. This was confirmed by gel filtration chromatography (not shown). Covalent cross-linking between MyoD and the CaBPs occurred only in the presence of Ca^{2+} (lanes 3). When MyoD was incubated with CaM in the presence of Ca^{2+}, the MyoD−CaM complexes were multiples and migrated as heterodimers or higher molecular weight complexes. However, when MyoD was incubated with S100a plus Ca^{2+}, the cross-linked MyoD oligomers disappeared. The MyoD protein now migrated as a heterodimer complexed with one S100α subunit and, unexpectedly, as a MyoD monomer. Together these data suggest that S100a in its Ca^{2+}-bound state prevented MyoD aggregation more efficiently than CaM, but also that the nature of the S100−MyoD complex rendered it less susceptible to covalent cross-linking.

The absence of cross-linked products between CaBPs with MyoD in the presence of EGTA contrasts with the affinity chromatography results (Figure 2) that revealed Ca^{2+}-independent interaction between MyoD and the CaBP-Sepharose columns. Several hypotheses could explain that discrepancy: (i) The high local concentration of CaBP on the Sepharose colum might contribute to Ca^{2+}-independent interaction with low-affinity sites on the MyoD molecule. (ii) When covalently coupled to the Sepharose matrix in the presence of Ca^{2+}, a population of CaBP protein might retain a Ca^{2+}-bound like conformation even in the presence of EGTA. (iii) The hydrophobic nature of the interactions between the molecules might prevent the accessibility of the hydrophilic cross-linker to the interacting domains.

S100a and CaM Inhibit MyoD Phosphorylation by PKC, but Phosphorylation of MyoD by PKC Does Not Antagonize Its Binding to S100a and CaM. Studies to compare the effects of S100a and CaM on the phosphorylation of MyoD by PKC revealed that both CaBPs inhibited stoichiometrically MyoD phosphorylation (Figure 4A). The observed inhibition of the PKC-dependent phosphorylation of MyoD involved the interaction of the CaBPs with the substrate rather than with the kinase itself since CaBPs, at the concentration used, inhibited neither the autophosphorylation of PKC nor the phosphorylation of H1 histone, an effective substrate for PKC (Baudier et al., 1987).

The Ca^{2+}-dependent association of MyoD with CaM and S100a was not regulated by phosphorylation. When MyoD was phosphorylated by PKC, it bound to CaM- and S100a-Sepharose columns in the presence of Ca^{2+} and was not dislodged by repeated salt washes. The phosphorylated MyoD eluted when Ca^{2+} was chelated (Figure 4B). As observed with the non-phosphorylated MyoD, residual bound ^{32}P-labeled MyoD eluted from the S100a column with 5 M guanidinium chloride (not shown).

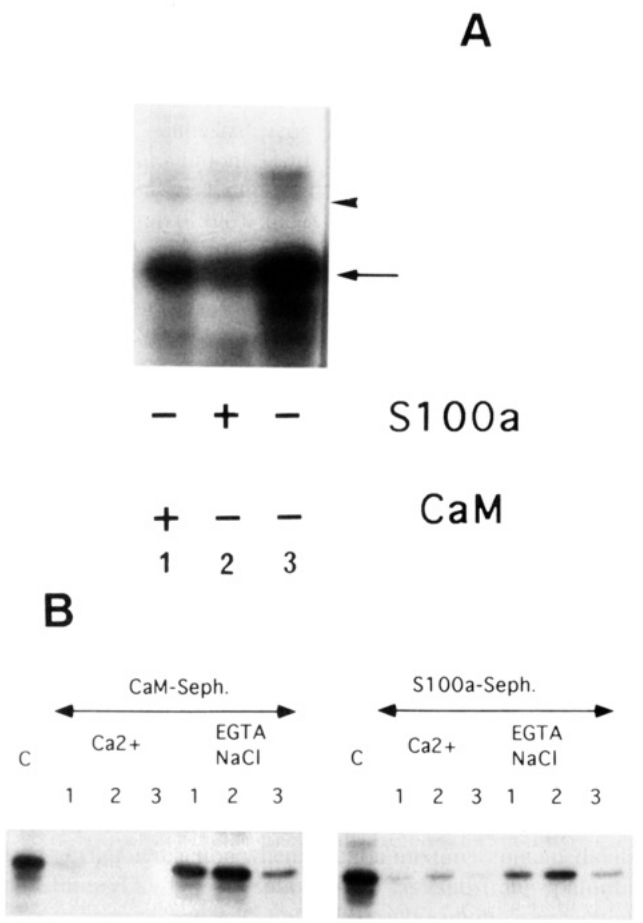

FIGURE 4: S100a and CaM inhibit MyoD phosphorylation by PKC. (A) Autoradiograms showing the effects of S100a and CaM on PKC phosphorylation of MyoD. Phosphorylation was performed in the presence of 0.3 mM $CaCl_2$. The reaction time was 5 min, and the S100a:MyoD (lane 2) and CaM:MyoD (lane 1) ratios were 1 and 2, respectively. The arrow indicates the position of the MyoD monomer; the arrowhead indicates the position of the autophosphorylated PKC. (B) PKC phosphorylation did not antagonize MyoD binding to S100a. MyoD (0.1 mg) was ^{32}P-labeled by phosphorylation with PKC for 30 min at 30 °C in standard assay conditions. The phosphorylated protein was then mixed with a 5× excess of non-phosphorylated protein in 1 mL of buffer A plus 0.5 mM $CaCl_2$. The protein solution was separated into two batches (0.5 mL each), which were applied separately on a CaM- or S100a-Sepharose column (0.7 mL) as described in the caption of Figure 1. The columns were first washed with 10 mL of buffer A plus $CaCl_2$ and then with buffer A containing 4 mM EGTA plus 0.5 M NaCl. One-milliliter fractions were collected, and the first three fractions were analyzed by gel electrophoresis and autoradiography.

CaM and S100a Inhibit DNA Binding to MyoD. Because the predicted S100a and CaM binding domain on MyoD corresponded to the basic helix I motif on the bHLH domain, and because that domain was directly implicated in DNA binding (Fairman et al., 1993), we decided to determine whether the association of S100a or CaM with MyoD may interfere with DNA binding to MyoD. For that purpose we tested the effects of S100a and CaM on the binding of MyoD to a target 25-bp oligonucleotide probe from the MCK enhancer containing the consensus binding site (CA--TG) of myogenic bHLH proteins in a gel mobility shift assay. When MyoD was mixed with ^{32}P-labeled DNA probe and electrophoresed on a native 5% polyacrylamide gel, a prominent mobility shift of the probe with 10−60 ng of MyoD was observed (Figure 5). When S100a (1.5 μM) and CaM (2 μM) were first added to the MyoD protein in the

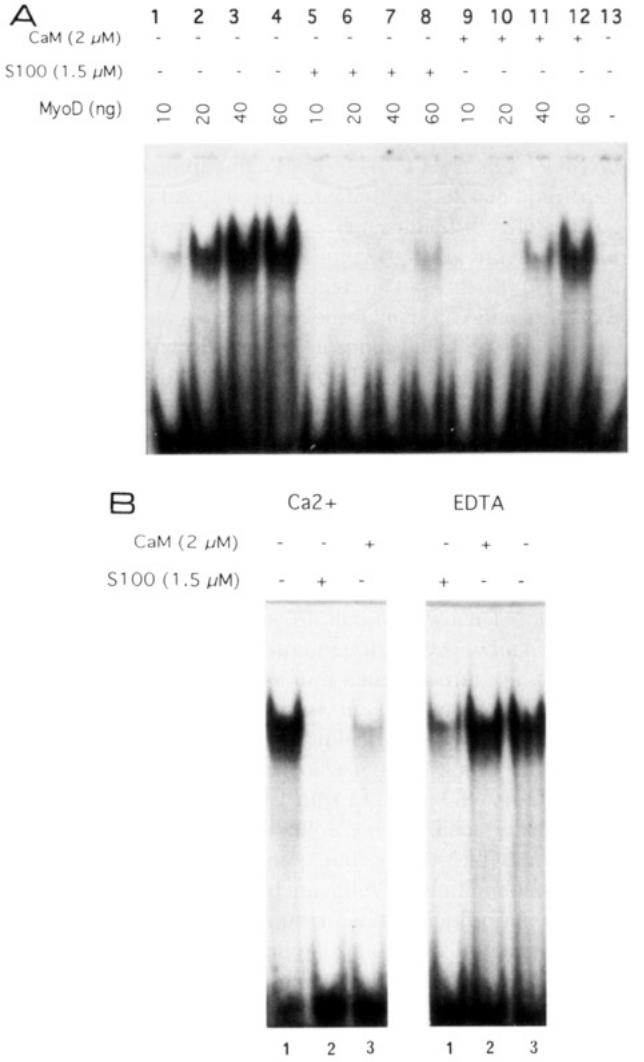

FIGURE 5: S100a and CaM antagonize DNA binding to MyoD. (A) Increasing amounts (10−60 ng) of a diluted preparation of MyoD (0.2 μM) were incubated in binding buffer, in the absence (lanes 1−4) or presence of S100a (1.5 μM) (lanes 5−8) or CaM (2 μM) (lanes 9−12) plus 0.1 mM $CaCl_2$, with 1 ng of ^{32}P-labeled DNA probe. The mixture was run on a 5% non-denaturating polyacrylamide gel as described in Materials and Methods. In lane 13 is the DNA probe. (B) Comparison of the effect of Ca^{2+} (0.1 mM) and EDTA (0.1 mM) on the antagonistic effect of S100a (1.5 μM) and CaM (2 μM) on DNA (1 ng) binding to MyoD (60 ng).

presence of Ca^{2+}, they each inhibited DNA binding to MyoD to a different extent (Figure 5A). S100a was more efficient than CaM. The effect of CaM was strictly Ca^{2+}-dependent, whereas the inhibitory effect of S100a on DNA binding also occurred in the presence of EGTA, although to a much lesser extent than in the presence of calcium (Figure 5B).

Binding of S100a and CaM to the MyoD bHLH Domain. The experiments described above strongly suggested to us that the bHLH domain on MyoD could function as a CaM/S100 binding domain. To confirm that hypothesis, we studied interactions between a bacterial recombinant MyoD bHLH peptide (residues 102−166 of the mouse MyoD protein) with CaM and S100a.

The recombinant bHLH domain binds to calmodulin-Sepharose (Figure 6) and to S100a-Sepharose (not shown) columns in a calcium-dependent manner. Final purification of the MyoD bHLH peptide was achieved by reverse-phase FPLC (see Materials and Methods). MyoD bHLH was 95% pure after this procedure when analyzed by 13% SDS−

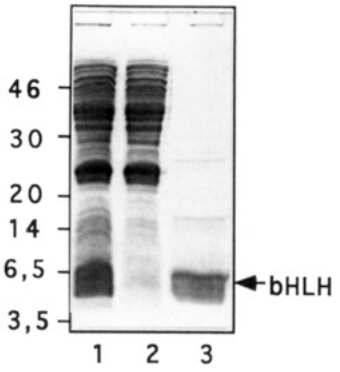

FIGURE 6: Ca^{2+}-dependent affinity chromatography of recombinant MyoD bHLH on CaM-Sepharose column. The 80% ammonium sulfate cell extract containing recombinant MyoD bHLH in 20 mM Hepes, pH 7.5, 0.5 M NaCl, and 10 mM DTT (buffer A) plus 0.5 mM $CaCl_2$ was applied on a CaM-Sepharose column equilibrated with buffer A plus 0.5 mM $CaCl_2$. The column was first washed with 10 column volumes of the equilibrating buffer and then with buffer A containing 2 mM EGTA. The loading sample (lane 1), the flow-through fraction (lane 2), and the protein eluted with EGTA-containing buffer (lane 3) were analyzed by 17% SDS–PAGE. In the left margin are the molecular weight standards ($\times 10^{-3}$).

PAGE (Figure 7A, lane 3). In Figure 7A are also shown the migration patterns of CaM (lane 1) and S100a (lane 2).

Native gel electrophoresis was then used to monitor complex formation between CaBPs and MyoD–bHLH (Figure 7B–D). In native PAGE, MyoD bHLH did not enter the gel due to the basic nature of the peptide (panel C, lane 3). When MyoD bHLH was mixed with increasing amounts of CaBPs in the presence of EGTA and subjected to 13% PAGE (panel B), the bHLH protein still did not penetrate the gel and the migration of the S100a (lanes 1–3) and CaM (lanes 4–6) was not modified. In the presence of Ca^{2+}, the electrophoretic mobility of both CaBPs decreased (panel C, lanes 1 and 4). The smear that characterizes S100a (lane 1) was due to conformational changes induced upon Ca^{2+} binding which destabilized the quaternary protein structure, leading to subunit dissociation (Baudier et al., 1986a). When CaBPs were mixed with MyoD bHLH in the presence of Ca^{2+}, complex formation between CaBPs and the MyoD bHLH could be observed that resulted in an upward shift of the CaBPs bands (Panel C, lanes 2 and 5). The binding of CaBPs to bHLH was saturable around a molar ratio of 1 CaBP:1 bHLH (panel D). Note that, at a molar ratio of 0.5 S100a:1 bHLH , heterogeneity in the migration of the S100a–bHLH complexes could be observed (panel C, lane 2, and panel D, lane 1). This heterogeneity suggested a possible sequential binding of the dissociated S100α subunit to bHLH molecules.

We next attempted to determine the affinity of the MyoD bHLH domain for CaM. Dansyl calmodulin (CaM-DANS) has proven to be very useful for determining the affinity of peptides for CaM (Graff et al., 1989). We therefore examined the binding of MyoD bHLH peptide to CaM-DANS. Figure 8A shows that, upon mixing bHLH (2 μM) with Ca^{2+}-bound CaM-DANS (200 nM), the peptide produced an increase in the fluorescence of the Ca^{2+}-bound CaM-DANS and a shift of the maximum of emission from 500 to 475 nm. If EGTA was then added to the bHLH–Ca^{2+}-bound CaM-DANS mixture, the fluorescence spectrum of the CaM-DANS became identical to that of apo-CaM-DANS. These results indicated that MyoD bHLH, under

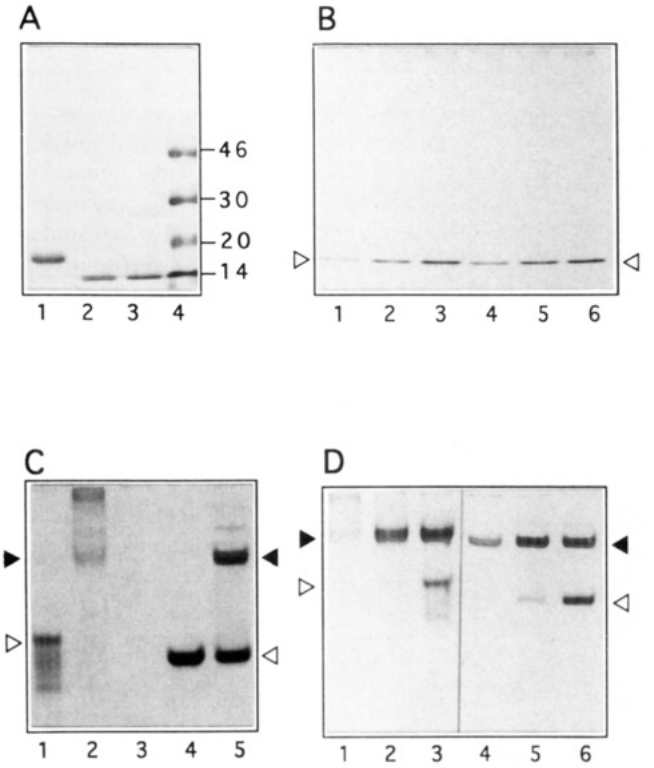

FIGURE 7: Ca^{2+}-dependent complex formation of MyoD bHLH with CaM and S100a. Panel A shows the migration of purified CaM (lane 1), S100a (lane 2), and MyoD bHLH (lane 3) on a 13%-SDS PAGE gel. Panel B shows the migration in native 13% PAGE plus 1 mM EGTA of MyoD bHLH mixed with S100a at molar ratios of 0.5 (lane 1), 1 (lane 2), and 2 (lane 3) or mixed with CaM at molar ratios of 0.5 (lane 4), 1 (lane 5), and 2 (lane 6). Panel C shows the migration in native 13% PAGE plus 0.5 mM $CaCl_2$ of S100a (lane 1), S100a plus MyoD bHLH at a molar ratio of 0.5 (lane 2), MyoD bHLH (lane 3), CaM (lane 4), and CaM plus MyoD bHLH at a molar ratio of 2 (lane 5). Panel D shows the migration in native 13% PAGE plus 0.5 mM $CaCl_2$ of MyoD bHLH mixed with S100a at molar ratios of 0.5 (lane 1), 1 (lane 2), and 2 (lane 3) or mixed with CaM at molar ratios of 0.5 (lane 4), 1 (lane 5), and 2 (lane 6). In panels B, C, and D, open arrowheads point to CaBPs and solid arrowheads point to MyoD bHLH–CaBP complexes. Differences in protein mobilities between panels C and D are due to differences in the migration time.

the conditions of the experiment, interacted with CaM exclusively in the presence of Ca^{2+}. Figure 8B shows the fluorescence increase that occurred when 40, 100, 200, and 400 nM Ca^{2+}-bound CaM-DANS was titrated with bHLH peptide. In every case, the peptide produced a 2.3-fold increase in the fluorescence of CaM-DANS at 475 nm with apparent dissociation constants (K_ds) that depended on the concentration of CaM-DANS. Figure 8C shows a plot of the K_d as a function of the concentration of CaM-DANS titrated. The data were analyzed by linear regression (r = 0.997), which extrapolated to a K_d around 20 nM at zero CaM-DANS concentration.

To estimate the affinity of the bHLH peptide for S100a protein, we studied the ability of S100a to compete with CaM-DANS in binding to MyoD bHLH peptide (Figure 8D). In these experiments CaM-DANS (100 or 200 nM) was first incubated with a saturating amount of bHLH peptide (0.5 or 1 μM, respectively). A 2.3-fold increase in CaM-DANS fluorescence at 475 nm was observed in both cases. We then analyzed the effect of increasing concentrations of S100a on the CaM-DANS fluorescence. By competing with CaM-DANS in binding to bHLH, S100a abolished totally the

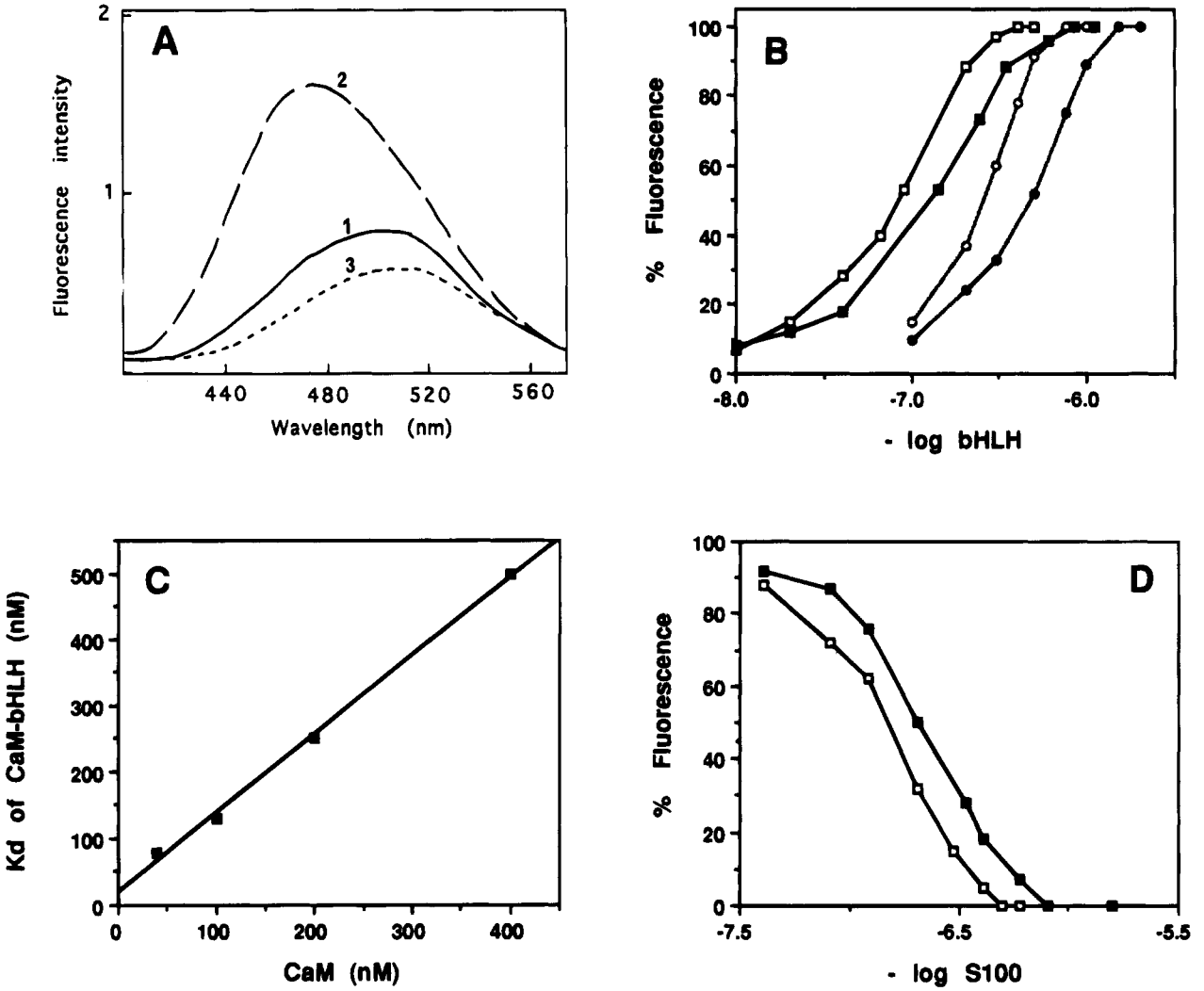

FIGURE 8: Binding of MyoD-bHLH to dansylcalmodulin. Panel A shows the fluorescence spectra of 200 nM CaM-DANS, combined with 0.1 mM $CaCl_2$ (curve 1), 2 μM MyoD bHLH and 0.1 mM $CaCl_2$ (curve 2), or 2 μM MyoD bHLH and 1 mM EGTA (curve 3). In panel B, the fluorescence increase in Ca^{2+}–CaM-DANS is shown as a function of added MyoD bHLH for 40 (□), 100 (■), 200 (○), and 400 nM (●) CaM-DANS. Panel C shows a plot of the apparent K_d of CaM-DANS/peptide binding versus the concentration of CaM-DANS being titrated. These data were analyzed by linear regression with a straight line plot (r = 0.997), which intercepted the y axis (zero CaM concentration, x = 0) at 20 nM. Panel D shows titrations of the S100a-mediated inhibition of CaM-DANS fluorescence complexed to MyoD bHLH under two different sets of conditions: (□) 100 nM CaM-DANS plus 500 nM MyoD-bHLH; (■) 200 nM CaM-DANS plus 1 μM MyoD bHLH. In panels B and C, each point represents the average of duplicate experiments.

bHLH-dependent increase in CaM-DANS fluorescence. We also performed controls to show that S100a had by itself no effect on the CaM-DANS fluorescence. S100a-mediated inhibition of CaM-DANS fluorescence was maximal around 0.6 mol of S100a per mol of MyoD bHLH. This suggested that each S100α subunit might interact with one bHLH peptide and that the affinity of the S100a for the bHLH peptide was at least 1 order of magnitude higher than the affinity of CaM for bHLH. The higher affinity of the bHLH peptide for S100a corroborated the observation that S100a exerts a stronger inhibition on DNA binding to MyoD compared to CaM (Figure 5).

Phosphorylation of MyoD-bHLH by PKC. The phosphorylation of MyoD bHLH by PKC from a commercial source was rapid and showed an apparent stoichiometry of 0.8 mol of phosphate incorporated per mol of bHLH (Figure 9A). This peptide was an excellent substrate for phosphorylation by PKC with a K_m of 0.8 μM (Figure 9B). The analysis of the phosphorylated amino acid residues (see Materials and Methods) revealed that the released radioactivity coincided with the identification of Thr 115, indicating that it is the major phosphorylated amino acid (Figure 9C). Thr 105 and Thr 106 were also phosphorylated but to a much lesser extent. In the presence of an equimolar amount of CaBPs the MyoD bHLH phosphorylation was severely inhibited (Figure 9D).

MyoD Co-Immunoprecipitates with S100a from H9c2 Cells Extracts. H9c2 cells, a clonal muscle cell line from rat heart exhibiting properties of skeletal muscle, differentiate into myotubes under low serum conditions (Kimes & Brandt, 1976). This cell line expressed both S100a mRNA and protein as revealed by Northern blot analysis of polyA mRNA and Western blot analysis of crude cell extract (data not shown). Western blot analysis also revealed that our S100a antiserum did cross react with three others minor proteins (not shown). H9c2 cells also expressed MyoD protein (see below). To compare the cellular localization of MyoD and S100a, exponentially growing H9c2 cells were fixed and immunostained with polyclonal antibodies against S100a or MyoD. In both cases the immunoreaction products were found in high density in the cell nuclei, but immu-

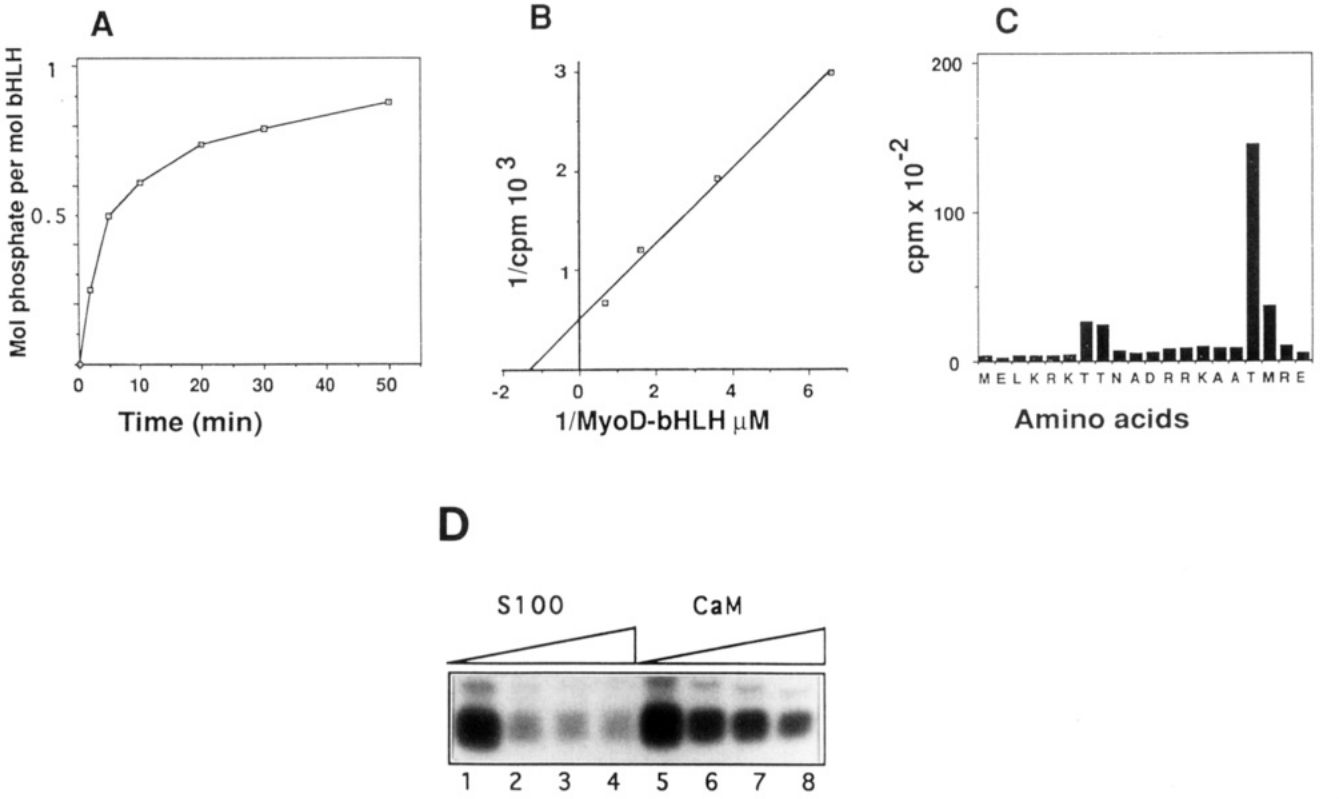

FIGURE 9: Phosphorylation of the MyoD-bHLH by PKC. Panel A: Stoichiometry of MyoD bHLH phosphorylation by PKC. MyoD bHLH (40 μg/mL) was incubated with PKC from commercial sources (0.1 μg/mL) for different periods of time. Panel B: Double-reciprocal plot of the phosphorylation of MyoD bHLH by PKC. In panels A and B, each point represents the average of duplicate determinations. Panel C: Radiosequencing of MyoD bHLH phosphorylated by PKC. The sequence of the first 20 amino acids of the MyoD bHLH peptide and the corresponding release of radioactivity are shown. Panel D: Inhibition of MyoD bHLH phosphorylation by S100a and CaM. MyoD bHLH at a concentration of 5 μM was mixed with increasing concentrations of S100a or CaM. Lanes 1 and 5, no CaBPs; lanes 2 and 6, 5 μM CaBPs; lanes 3 and 7, 10 μM CaBPs; lanes 4 and 8, 15 μM CaBPs. The phosphorylation reactions were carried out for 20 min at 30°C. The MyoD bHLH protein was analyzed by 17% SDS−PAGE followed by autoradiography of the gel.

noreactivity was also located in the cytoplasm (Figure 10A). A punctate staining pattern was observed in the cytoplasm of the cells with the two antisera. The specificity of the cytoplasmic immunoreactivities given by the two antibodies was confirmed by the fact that the immunoreactivities totally disappeared when the immunsera were first incubated with the purified proteins. Although the nuclear staining given by the MyoD antiserum can also be considered specific, the nuclear staining given by the S100a antiserum should be considered with caution since it was not totally suppressed after incubation of the immune serum with the purified protein. Nuclear staining with affinity-purified S100a antibodies has also been observed in adult skeletal muscle, although the bulk of the protein was cytoplasmic (Haimoto & Kato, 1987). A more recent report by Zimmer and Landar (1995) showed that, in skeletal muscle L6 cell line, S100a immunoreactivity was predominantly in the cytoplasm and exhibited a punctate staining pattern similar to that in H9c2 cells.

Definitive proof that S100a interacted with MyoD in myoblasts required co-immunoprecipitation of the two proteins. A two-step immunodetection procedure was therefore developed to investigate the interaction of MyoD with the S100a in H9c2 cell extracts (Figure 10B). Three distinct protein bands that migrated between the light and heavy chains of rabbit IgG and cross reacted with anti-mouse IgG were revealed in the MyoD immunoprecipitate (lane 2). That electrophoretic heterogeneity of the immunoprecipitated MyoD also has been observed previously, and probably corresponds to different phosphorylation states of the protein (Tapscott et al., 1988). The MyoD-like protein bands were clearly distinguishable in the S100a immunoprecipitate (lane 3) but not in controls (lanes 1 and 4), strongly suggesting that they coprecipitated with the S100a. It is noteworthy that the faster moving bands immunoprecipitated preferentially with the S100a in the presence of calcium, suggesting that the most abundant MyoD protein species, with lower electrophoretic mobility, has reduced affinity for S100a. That MyoD species could correspond to a hyperphosphorylated form of the protein (Mitsui et al., 1993). It is noteworthy that *in vitro* phosphorylation of MyoD by CKII, which induced a decrease in the protein electrophoretic mobility, also decreased the affinity of the protein for S100a. Phosphorylation of MyoD by CKII inhibited the Ca^{2+}-dependent binding of MyoD to an S100a-Sepharose column (C. Cochet, O. Filhol, and J. Baudier, unpublished data).

DISCUSSION

Interactions of MyoD and MyoD bHLH with Calmodulin and S100a. In this study we have confirmed the prediction that MyoD is a PKC substrate that interacts with the CaM and S100 proteins and that the multifunctional basic α-helix I domain of the bHLH motif in MyoD is directly involved in the Ca^{2+}-dependent interaction with CaBPs.

The affinity of the MyoD bHLH domain for CaM, around 20 nM, is 1 order of magnitude lower than that found for the highest affinity CaM-dependent enzymes, but is similar

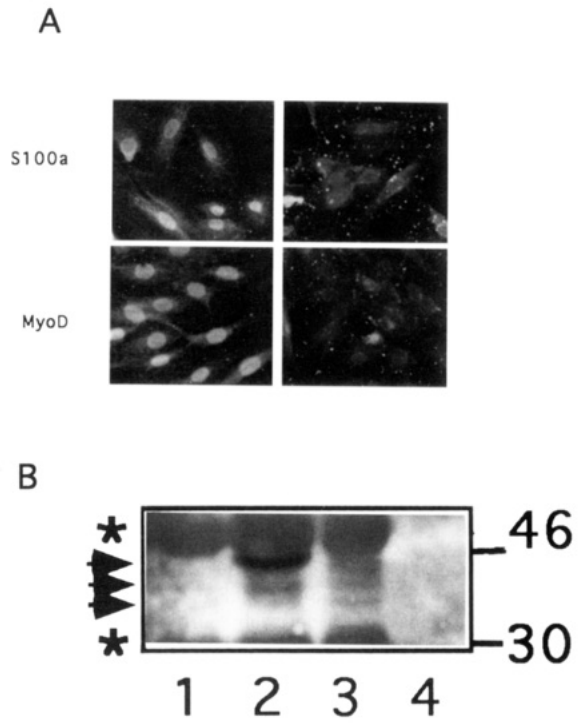

FIGURE 10: Cellular Interaction between S100a and MyoD. (A) Immunofluorescence localization of S100a and MyoD-like immunoreactivities in H9c2 cells. Left column, H9c2 cells labeled with S100a or MyoD antisera without competition. Right column, H9c2 cells labeled with S100a or MyoD antisera competed with S100a or MyoD proteins. (B) Co-immunoprecipitation of MyoD with S100a. Exponentially growing H9c2 cells were lysed in buffer containing calcium, and the S100a and MyoD were immunoprecipitated with rabbit polyclonal antibodies against S100a (lane 3) or against MyoD (lane 2). Rabbit polyclonal antibodies against the brain-specific protein neuromodulin (lane 1) or protein A alone (lane 4) were used as controls. The immunoprecipitates were solubilized in 0.5% SDS, run on a 10% SDS−PAGE gel, and transferred onto a nitrocellulose blotting membrane. The immunoprecipitated MyoD was then revealed with a mouse monoclonal antibody against MyoD and an anti-mouse IgG coupled to horseradish peroxidase. The ECL system was used to visualize the immune complexes. Arrows point to three distinct protein bands that react specifically with monoclonal antibody against MyoD. Stars indicate positions of the light and heavy chains of rabbit IgG, which cross reacted with anti-mouse IgG. In the right margin are the positions of molecular weight standards ($\times 10^{-3}$).

to that found for CaM-dependent enzymes such as adenylyl cyclase (Tang et al., 1991). This high nanomolar affinity remains physiologically significant since the concentration of calmodulin in mammalian tissues varies between 2 and 30 μM (Carafoli, 1987). The relative reduced affinity of the bHLH domain for CaM compared to CaM binding domains so far identified in high-affinity target enzymes could be explained by structural differences between these two classes of binding sites. The pattern of basic residues required for binding of the carboxyl-terminal domain of CaM to target peptides is conserved in the MyoD α helix I. The pattern of residues for the binding of the amino-terminal domain of CaM is less conserved on MyoD, in particular, two hydrophobic residues (residues 9 and 18) that may stabilize the CaM-target complexes (Ikura et al., 1992; Bagchi et al., 1992) are changed to hydrophilic residues in the MyoD proteins. This may lead to a reduced affinity between MyoD and CaM compared to CaM-target enzymes.

Although the mode of interaction between the S100 protein and target peptide is not as well documented as that for CaM, similarities between S100 and CaM in their interaction with model target peptide for CaM have been reported (Baudier et al., 1987). It is thus likely that the CaM binding domain on MyoD may also be targeted by S100a. The S100 proteins exist as dimers in solution with the two subunits in an antiparallel arrangement (i.e., the H-NMR spectrum of the protein dimer corresponds to that of a single subunit). The S100 subunits are predicted to form one globular domain with two Ca^{2+}-binding sites, corresponding to half of the CaM molecule (Szebeny & Moffat, 1986). Competition studies showed that total dissociation of the MyoD bHLH−CaM-DANS complex was achieved at a MyoD bHLH:S100a ratio of 0.6. Thus, in the presence of Ca^{2+}, one S100α subunit might be able to bind to one MyoD bHLH molecule. DNA binding competition assays using the entire MyoD molecule revealed clearly that the S100a protein was more efficient in inhibiting MyoD−DNA binding than CaM, suggesting a higher MyoD affinity for S100a than for CaM. We confirmed a higher affinity of at least an order of magnitude of the MyoD bHLH domain for S100a than for CaM in the presence of Ca^{2+} from binding competition experiments between CaM-DANS and S100a. The affinity of MyoD bHLH for S100a is likely in the low nanomolar range and makes plausible the interaction of S100a with myogenic proteins in muscle cells, since in developing and adult skeletal and heart muscles S100a is expressed at very high levels (Kato et al., 1986; Haimoto & Kato, 1987, 1988; Zimmer, 1991). The S100a contents in human skeletal and heart muscle are 1 μg/mg soluble protein and 1.8 μg/mg soluble protein, respectively (Kato et al., 1986). In proliferating L6 myoblasts S100a content is 35 ng/mg total protein (Zimmer & Landar, 1995). In favor of an *in vivo* interaction between S100a and MyoD are also the observations that S100a- and MyoD-like immunoreactivities colocalize in the cytoplasm of H9c2 cells and that a significant amount of MyoD-like immunoreactivity is recovered in the S100a immunoprecipitate from crude H9c2 cell extract in the presence of calcium.

Phosphorylation of MyoD and MyoD-bHLH by PKC. The observed *in vitro* phosphorylation of MyoD and MyoD bHLH by PKC on Thr 115, which is homologous to Thr 87 on myogenin, confirmed the function of the conserved basic region of myogenic bHLH domain as a PKC phosphorylation site domain (Li et al., 1992). As observed with myogenin, phosphorylation of MyoD by PKC inhibits MyoD−DNA binding *in vitro* (data not shown). The K_m value of 0.8 μM we found for the PKC phosphorylation of MyoD bHLH is 2 orders of magnitude lower than that found for a synthetic peptide corresponding to amino acids 82−91 in the basic domain of myogenin (RRRAATLREK; K_m 77.4 μM) (Li et al., 1992). Therefore, the basic region (b) of the bHLH domain is not sufficient for optimal phosphorylation of the protein, and probably other amino acids within the helix I domain contribute to the interaction of the protein with the activated phospholipid-bound kinase. Through binding to the MyoD bHLH domain, CaM and S100a inhibit PKC phosphorylation of Thr 115, although that residue is not included in the predicted CaBP binding site. We propose that CaBPs inhibits MyoD phosphorylation by PKC because they sterically hinder the interaction of MyoD bHLH with the phospholipid-bound PKC, and that residues within the helix I motif, involved in CaBP binding, are essential for the specificity of the phosphorylation of the MyoD bHLH

by PKC. That the phosphorylated Thr 115 is apart from the predicted CaBP binding domain also explains why the phosphorylated MyoD is still able to bind to CaBP-Sepharose columns (Figure 4B). In this respect MyoD behaves differently from other CaM binding PKC substrates of the MARCKS and neurogranin/neuromodulin (Ng/Nm) families. For these PKC substrates the phosphorylated residues are located within the CaM binding domains, and the binding to CaM is antagonized by phosphorylation (Mc Ilroy et al., 1991; Li & Aderem, 1992; Alexander et al., 1988).

It is noteworthy that, in contrast to MyoD, myogenin, or MyoD bHLH, PKC phosphorylated the myogenic MRF4 protein *in vitro* preferentially at Ser 220 and Ser 221. Ser 220 and 221 on MRF4 are located within a peptide sequence that has no homology with the consensus PKC phosphorylation site domain and are also phosphorylated by PKA, arguing against a specific phosphorylation of these residues by PKC. The weak *in vitro* phosphorylation of MRF4 on the conserved Thr 99 compared to MyoD, myogenin, or MyoD bHLH may result from differences in the protein conformational status. We indeed have observed that, upon storage, properties of the MyoD and MyoD bHLH proteins were altered. PKC phosphorylation stoichiometry and DNA binding activities drastically decreased. We attributed these changes to the formation of stable protein aggregates.

Myogenic Proteins: A New Class of CaM/S100-Binding PKC Substrate? In eukaryotic cells, calcium, as a second messenger, plays a pivotal role in the transduction of extracellular stimulation linked to cell proliferation and differentiation. Ca^{2+} participates in the activation of Ca^{2+}-dependent enzymes, such as PKC, and in the activation of CaBPs. An interdependence is suspected between the Ca^{2+}-transduction pathways utilizing PKC and the CaBPs. Indeed, a number of cytosolic PKC substrates have been identified that are able to interact with the CaBP, CaM, and S100 proteins, in a Ca^{2+}-dependent or Ca^{2+}-independent manner. These include the MARCKS protein family (Aderem, 1992; Blackshear, 1993) and the Ng/Nm family (Alexander et al., 1988; Baudier et al., 1992). MARCKS interacts with CaM in the presence of Ca^{2+} with an affinity in the low nanomolar range (Graff et al., 1989), whereas Ng/Nm interacts with CaM in the absence of Ca^{2+} with an affinity in the micromolar range (Alexander et al., 1988). Members of each family are characterized by a multifunctional conserved motif of 17−20 amino acids that correspond to the PKC phosphorylation site domain and the CaM binding domain. Here we characterized the multifunctional MyoD bHLH domain, that is conserved within all the members of myogenic proteins, as a PKC phosphorylation domain that interacts with CaM and the S100a protein abundant in muscle. We can thus predict that the other myogenic proteins will also be phosphorylated by PKC and will interact with the CaBPs, thus forming a new class of CaM/S100 binding PKC substrate.

It has been shown that bFGF inhibits myogenesis by inactivating myogenic proteins, possibly through a PKC-dependent pathway. FGF induces phosphorylation of the PKC phosphorylation site on myogenin (Thr 87) that is homologous to Thr 115 in MyoD. The phosphorylation of myogenin on Thr 87 mediates repression of myogenin activity (Li et al., 1992). The presence of this phosphorylation site in all myogenic bHLH proteins suggests that it may represent a conserved target for negative control of these proteins' functions via regulated phosphorylation. However, the relevance of a direct phosphorylation of all myogenic proteins by PKC is somewhat controversial. Recent studies have shown that MRF4 is in fact only weakly phosphorylated by PKC at the conserved threonine residue (Thr 99) *in vitro* and *in vivo*, and although Thr 99 is essential for myogenic activity, its state of phosphorylation does not play a major role in regulating MRF4 activity (Hardy et al., 1993). Given the reported differences on the role of phosphorylation by PKC of myogenin (Thr 87) and MRF4 (Thr 99) activities, it is actually difficult to assign with certainty a role for that mode of phosphorylation in myogenesis. That the CaBPs, CaM or S100a, could participate in regulating myogenic protein phosphorylation by PKC *in vivo* is, however, a reasonable hypothesis that requires to be confirmed. Because, in contrast to CaM, the S100a protein is mainly cytoplasmic in myoblasts and in muscle cells, one can envision that the calcium-dependent interaction of myogenic proteins with S100a could serve to modulate their phosphorylation by calcium-activated PKC, and/or other kinases, in the cytoplasm prior to translocation into the nucleus.

Finally, Corneliussen et al. (1994) recently reported that CaM can also directly interact with bHLH domain of some other bHLH transcription factors. This group also reported that the Ca^{2+} ionophore, ionomycin, selectively inhibits transcriptional activation of CaM-sensitive bHLH proteins, implying that Ca^{2+} can directly modulate bHLH proteins through their interaction with CaM. Surprisingly, MyoD transcriptional activity was poorly affected by the Ca^{2+} ionophore in a transfection assay that utilizes Burkitt's lymphoma cells. This suggests that interaction between MyoD and CaM is not sufficient to modulate MyoD transcriptional activities in this cell line. Our finding that the myogenic bHLH domain can be targeted by another calcium-dependent regulator, the S100a protein, with higher affinity than CaM, suggests that not only CaM may contribute to the Ca^{2+}-dependent regulation of bHLH proteins; proteins of the S100 family could also participate in the regulation of individual bHLH transcription factors possibly in a cell-specific dependent manner.

ACKNOWLEDGMENT

We thank Dr. S. Khoshbin for setting up the DNA band shift assay; Dr. O. Filhol, Dr. C. Cochet, and Dr. M. Doré for providing us with purified CKII and cdc2 kinase; Dr. M. Buckingham and Dr. C. Hoemann for critical reading of the manuscript; Ms. M. P. Brocard for technical assistance, and Ms. M. Vinçon for amino acid sequence analysis.

REFERENCES

Aderem, A. (1992) *Cell 71*, 713−716.

Albert, K. A., Wu, W. C. S., Nairn, A. C., & Greengard, P. (1984) *Proc. Natl. Acad. Sci. U.S.A. 81*, 3622−3625.

Alexander, K. A., Wakim, B. T., Doyle, G. S., Walsh, K. A., & Storm, D. R. (1988) *J. Biol. Chem. 263*, 7544−7549.

Apel, E., Litchfield, D. W., Clark, R. H., Krebs, E. G., & Storm, D. R. (1991) *J. Biol. Chem. 266*, 10544−10551.

Bagchi, I. C., Huang, Q., & Means, A. R. (1992) *J. Biol. Chem. 267*, 3024−3029.

Baudier, J., & Cole, R. D. (1988) *J. Biol. Chem. 263*, 5876−5883.

Baudier, J., & Gerard, D. (1986) *J. Biol. Chem. 261*, 8204−8212.

Baudier, J., Holtzcherer, C., & Gerard, D. (1982) *FEBS Lett. 148*, 231−234.

Baudier, J., Glasser, N., & Gerard, D. (1986a) *J. Biol. Chem. 261*, 8192−8203.
Baudier, J., Glasser, N., & Duportail, G. (1986b) *Biochemistry 25*, 6934−6941.
Baudier, J., Mochly-Rosen, D., Newton, A., Lee, S. H., Koshland, D. E., Jr., & Cole, R. D. (1987) *Biochemistry 26*, 2886−2893.
Baudier, J., Deloulme, J. C., Van Dorsselaer, A., Black,D., & Matthes, H. W. D. (1991) *J. Biol. Chem. 266*, 229−237.
Baudier, J., Delphin, C., Grunwald, D., Khochbin, S., & Lawrence, J. J. (1992) *Proc. Natl. Acad. Sci. U.S.A. 89*, 11627−11631.
Benezra, R., Davis, R. L., Lockshon, D., Turner, D. L., & Weintraub, H. (1990) *Cell 61*, 49−59.
Blackshear, P. J. (1993) *J. Biol. Chem. 268*, 1501−1504.
Braun, T., Buschhausen-Denker, G., Bober, E., Tannich, E., & Arnold, H. H. (1989) *EMBO J. 8*, 701−7709.
Carafoli, E. (1987) *Annu. Rev. Biochem. 56*, 395−433.
Corneliussen, B., Holm, M., Waltersson, Y., Onions, J., Hallberg, B., Thornell, A., & Grundstrom, T. (1994) *Nature 368*, 760−764.
Davis, R. L., Cheng, P. F., Lassar, A. B., & Weintraub, H. (1990) *Cell 60*, 733−746.
Deloulme, J. C., Sensenbrenner, M., & Baudier, J. (1989) In *Calcium Binding Protein in Normal and Transformed Cells* (Pochet, R., Lawson, E. M., & Heizmann, C. W., Eds.) pp 153−157, Plenum Publishing Corporation.
Engelkamp, D., Schafer, B. W., Erne, P., & Heizmann, C. W. (1992) *Biochemistry 31*, 10258−10264.
Engelkamp, D., Schafer, B. W., Mattei, G., Erne, P., & Heizmann, C. W. (1993) *Proc. Natl. Acad. Sci. U.S.A. 90*, 6547−6551.
Fairman, R., Beran-Steed, R. K., Anthony-Cahill, S. J., Lear, J. D., Stafford, W. F., III, Degrado, W. F., Benfield, P. A., & Brenner, S. L. (1993) *Proc. Natl. Acad. Sci. U.S.A. 90*, 10429−10433.
Fano, G., Full, S., Della Torre, G., Giambanco, I., Aisa, M. C., Donato, R., & Calissano, P. (1988) *FEBS Lett. 240*, 177−180.
Fitzsimons, D. P., Herring, B. P., Stull, J. T., & Gallagher, P. (1992) *J. Biol. Chem. 267*, 23903−23909.
Garin, J., Vinçon, M., Gagnon, J., & Vignais, P. V. (1994) *Biochemistry 33*, 3772−3777.
Graff, J. M., Young, T. N., Johnson, J. D., & Blackshear, P. J. (1989) *J. Biol. Chem. 264*, 21818−21823.
Hagiwara, M., Ochiai, M., Owada, K., Tanaka, T., & Hidaka, H. (1988) *J. Biol. Chem. 263*, 6438−6441.
Haimoto, H., & Kato, K. (1987) *J. Neurochem. 48*, 917−923.
Haimoto, H., & Kato, K. (1988) *Eur. J. Biochem. 171*, 409−415.
Hardy, S., Kong, Y., & Konieczny, S. F. (1993) *Mol. Cell. Biol. 13*, 5943−5956.
Herring, P. H. (1991) *J. Biol. Chem. 266*, 11838−11841.
Hilt, D. C., & Kligman, D. (1991) in *Novel Calcium-Binding Proteins: Fundamentals and Clinical Implications.* (Heizmann, C. W., Ed.) pp 65−103, Springer Verlag, Berlin.
Ikura, M., Clore, M. G., Gronenborn, A. M., Zhu, G., Klee, C. B., & Bax, A. (1992) *Science 256*, 632−638.
Ivanenkov, V. V., Gerke, V., Minin, A. A., Plessmann, U., & Weber, K. (1993) *Mech. Dev. 42*, 151−158.
Kato, K., Kimura, S., Haimoto, H., & Suzuki, T. (1986) *J. Neurochem. 46*, 1555−1560.
Kennelly, P. J., & Krebs, E. G. (1991) *J. Biol. Chem. 266*, 15555−15558.
Kimes, B. W., & Brandt, B. L. (1976) *98*, 367−381.
Kligman, D., & Hilt, D. C. (1988) *Trends. Biochem. Sci. 13*, 437−443.
Labourdette, G., & Mandel, P. (1978) *Biochem. Biophys. Res. Commun. 96*, 1702−1709.
Li, J., & Aderem, A. (1992) *Cell 70*, 791−801.
Li, L., James, G., Heller-Harrison, R., Czech, M. P., & Olson, E. (1992) *Cell 71*, 1181−1194.
Marshak, D. R., Watterson, D. M., & Van Eldik, L. (1981) *Proc. Natl. Acad. Sci. U.S.A. 78*, 6793−6797.
McIlroy, B. K., Walters, J. D., Blackshear, P. J., & Johnson, J. D. (1991) *J. Biol. Chem. 266*, 4959−4964.
Meador, W., Means, A. R., & Quiocho, F. A. (1992) *Science 257*, 1251−1255.
Merlie, J. P., Mudd, J., Cheng, T. S., & Olson, E. N. (1994) *J. Biol. Chem. 269*, 2461−2467.
Miner, J. H., & Wold, B. (1990) *Proc. Natl. Acad. Sci. U.S.A. 87*, 1089−1093.
Mitsui, K., Shirakata, M., & Paterson, B. M. (1993) *J. Biol. Chem. 268*, 24415−24420.
Olson, E. N. (1990) *Genes Dev. 4*, 1454−1461.
Pelosin, J. M., Vilgrain, I., & Chambaz, E. M. (1987) *Biochem. Biophys. Res. Commun. 147*, 382−391.
Persechini, A., Moncrief, N. D., & Kretsinger, R. H. (1989) *Trends Neurosci. 12*, 462−467.
Starovasnik, M. A., Blackwell, T. K., Laue, T. M., Weintraub, H., & Klevit, R. E. (1992) *Biochemistry 31*, 9891−9903.
Studier, F. W., & Moffatt, B. A. (1986) *J. Mol. Biol. 189*, 113−130.
Szebenyi, D. M. E., & Moffat, K. (1986) *J. Biol. Chem. 261*, 8761−8777.
Tang, W. J., Krupinski, J., & Gilman, A. G. (1991) *J. Biol. Chem. 266*, 8595−8605.
Tapscott, S. J., Davis, R. L., Thayer, M. J., Cheng, P. F., Weintraub, H., & Lassar, A. B. (1988) *Science 242*, 405−411.
Weintraub, H., Dwarki, V. J., Verma, I., Davis, R., Hollenberg, S., Snider, L., Lassar, A., & Tapscott, S. J. (1991) *Genes Dev. 5*, 1377−1386.
Wright, W. E., Sassoon, D. A., & Lin, V. K. (1989) *Cell 56*, 607−617.
Zimmer, D. B. (1991) *Cell Motil. Cytoskeleton 20*, 325−337.
Zimmer, D. B., & Landar, A. (1995) *J. Neurochem. 64*, 2727−2736.

BI942468I